1521-0111/98/6/677–685$35.00
MOLECULAR PHARMACOLOGY

https://doi.org/10.1124/molpharm.120.000061
Mol Pharmacol 98:677–685, December 2020

N-Terminal Targeting of Regulator of G Protein Signaling Protein 2 for F-Box Only Protein 44–Mediated Proteasomal Degradation[S]

Harrison J. McNabb, Stephanie Gonzalez, Christine S. Muli, and Benita Sjögren

Department of Medicinal Chemistry and Molecular Pharmacology, Purdue University, West Lafayette, Indiana

Received May 8, 2020; accepted September 17, 2020

ABSTRACT

Regulator of G protein signaling (RGS) proteins are negative modulators of G protein signaling that have emerged as promising drug targets to improve specificity and reduce side effects of G protein–coupled receptor–related therapies. Several small molecule RGS protein inhibitors have been identified; however, enhancing RGS protein function is often more clinically desirable but presents a challenge. Low protein levels of RGS2 are associated with various pathologies, including hypertension and heart failure. For this reason, RGS2 is a prominent example wherein enhancing its function would be beneficial. RGS2 is rapidly ubiquitinated and proteasomally degraded, providing a point of intervention for small molecule RGS2-stabilizing compounds. We previously identified a novel cullin-RING E3 ligase utilizing F-box only protein 44 (FBXO44) as the substrate recognition component. Here, we demonstrate that RGS2 associates with FBXO44 through a stretch of residues in its N terminus. RGS2 contains four methionine residues close to the N terminus that can act as alternative translation initiation sites. The shorter translation initiation variants display reduced ubiquitination and proteasomal degradation as a result of lost association with FBXO44. In addition, we show that phosphorylation of Ser^3 may be an additional mechanism to protect RGS2 from FBXO44-mediated proteasomal degradation. These findings contribute to elucidating mechanisms regulating steady state levels of RGS2 protein and will inform future studies to develop small molecule RGS2 stabilizers. These would serve as novel leads in pathologies associated with low RGS2 protein levels, such as hypertension, heart failure, and anxiety.

SIGNIFICANCE STATEMENT

E3 ligases provide a novel point of intervention for therapeutic development, but progress is hindered by the lack of available information about specific E3-substrate pairs. Here, we provide molecular detail on the recognition of regulator of G protein signaling protein 2 (RGS2) by its E3 ligase, increasing the potential for rational design of small molecule RGS2 protein stabilizers. These would be clinically useful in pathologies associated with low RGS2 protein levels, such as hypertension, heart failure, and anxiety.

Introduction

Regulators of G protein signaling (RGS) proteins play a key role as negative modulators of signaling through G protein–coupled receptors (Ross and Wilkie, 2000; Sjögren et al., 2010; Sjögren, 2017). They act by directly binding to active, GTP-bound α subunits of heterotrimeric G proteins and accelerating GTP hydrolysis, thereby reducing amplitude and duration of G protein–mediated signal transduction. As such, RGS proteins represent novel therapeutic targets. Although progress has been achieved in developing RGS inhibitors (Blazer et al., 2010, 2011; Turner et al., 2012), increasing rather than decreasing RGS protein activity would yield a more beneficial clinical outcome in several instances. A prominent example is demonstrated by RGS2. Low RGS2 protein levels are implicated in a wide variety of pathologies, including hypertension, heart failure (Tsang et al., 2010), prostate cancer (Cao et al., 2006), asthma (Holden et al., 2011; George et al., 2018), and anxiety (Oliveira-Dos-Santos et al., 2000). Thus, finding selective ways to increase RGS2 protein levels could have broad clinical implications. The effects of RGS2 on blood pressure regulation can be explained, at least in part, by its selectivity for $G\alpha_q$ that mediates vasoconstriction in response to angiotensin II, endothelin-1, and other hormones. Consequently, $RGS2^{-/-}$ mice are hypertensive and show prolonged responses to these vasoconstrictors (Heximer et al., 2003). In addition, mutations associated with hypertension in humans (Yang et al., 2005) display reduced protein expression (Bodenstein et al., 2007; Phan et al., 2017). We demonstrated that pharmacological enhancement of RGS2

This project has received support from the American Heart Association [15SDG21630002] and the Ralph W. and Grace M. Showalter Research Trust.
https://doi.org/10.1124/molpharm.120.000061.
[S] This article has supplemental material available at molpharm.aspetjournals.org.

ABBREVIATIONS: BRCA1, breast cancer type 1 susceptibility protein; CIP, calf intestinal alkaline phosphatase; co-IP, co-immunoprecipitation; CRL, cullin-RING ligase; DCM, dichloromethane; DMF, dimethylformamide; FBXO44, F-box only protein 44; Fmoc, fluorenylmethyloxycarbonyl; HA, hemagglutinin; HEK-293T, human embryonic kidney 293T; hTERT, human telomerase reverse transcriptase; PKC, protein kinase C; PL, ProLabel; RGS, regulator of G protein signaling; RIPA, radioimmunoprecipitation assay; RT, room temperature; S3A, Ser^3 to alanine; S3D, Ser^3 to aspartic acid; siRNA, small interfering RNA; Skp1, S-phase kinase-associated protein 1; UPS, ubiquitin-proteasomal system; WT, wild type.

protein levels correlates with increased function. Digoxin-mediated stabilization of RGS2 protein levels has functional effects on G protein–coupled receptor signaling, both in vitro and in vivo (Sjögren et al., 2012, 2016). Although these studies represented an important proof of concept for the therapeutic benefit of RGS2 protein stabilization, the mechanism for digoxin-mediated upregulation of RGS2 is not known. Thus, we have recently focused on the mechanisms by which RGS2 protein levels are regulated.

A key mechanism regulating RGS2 protein levels is rapid and constitutive degradation through the ubiquitin-proteasomal system (UPS) (Bodenstein et al., 2007; Sjögren et al., 2012). The UPS is a multistep process to mark proteins for degradation by coupling ubiquitin chains to a lysine residue on the target protein, through a concerted process facilitated by E1 (ubiquitin activating enzyme), E2 (ubiquitin conjugating enzyme), and E3 ligases. The ubiquitin chains are then recognized by the 26S proteasome for degradation. Specificity for certain substrate proteins is achieved by the large (>600 members) family of E3 ligases (Hershko and Ciechanover, 1998; Ravid and Hochstrasser, 2008). Dysfunction of the UPS can lead to accumulation of misfolded or aged proteins, cell cycle arrest, and uncontrolled cell proliferation (Hershko and Ciechanover, 1998; Pickart, 2001; Ciechanover and Schwartz, 2002; Ravid and Hochstrasser, 2008). As such, various pathologies, including cancer and cardiovascular disease, can be a result of UPS defects (Herrmann et al., 2004; Hoeller et al., 2006). Although inhibitors of the 26S proteasome, exemplified by bortezomib (PS-341; Velcade) and carfilzomib, have been employed as treatments for certain blood cancers (Adams et al., 1999; Adams, 2004), they are associated with severe side effects, including neuropathies, fatigue, and anemia. To avoid these side effects, our laboratory and others have explored the possibility of selectively targeting individual E3 ligase-substrate pairs (Ding et al., 2013; Park et al., 2013). This motivated our previous efforts to identify the cognate E3 ligase targeting RGS2 for degradation.

We identified a novel cullin-RING ligase (CRL) composed of cullin 4B, DNA damage-binding protein 1, and F-box only protein 44 (FBXO44) capable of degrading RGS2 (Sjögren et al., 2015). Within this complex, FBXO44 acts as the substrate-recognition component recruiting RGS2 to be ubiquitinated, thus identifying this interaction as a potential point of intervention for small molecule RGS2 stabilizers (Sjögren et al., 2015). Further elucidation of the RGS2-FBXO44 interaction interface would enable rational drug design of protein-protein interaction inhibitors that would act to protect RGS2 from degradation and enhance RGS2 protein levels. Therefore, in the current study we aimed to determine which region of RGS2 is recognized by FBXO44. RGS2 contains four N-terminal methionine residues that can act as alternative translation initiation sites (Met^1, Met^5, Met^{16}, and Met^{33}) (Gu et al., 2008), and the shorter translation variants resulting from initiation at Met^{16} or Met^{33} yield a protein that is protected from degradation (Kanai et al., 2017). Our hypothesis for the current study was therefore that FBXO44 would target RGS2 through a degron located in the very N terminus of the protein.

Materials and Methods

Materials. All chemicals were purchased from Millipore Sigma (St. Louis, MO) unless otherwise stated.

DNA Constructs. RGS2-FLAG wild-type (WT), M1, M5, M16, and M33 were a kind gift from Kendall Blumer, Washington University School of Medicine. RGS2-ProLabel (PL) M1, M5, M16, and M33 were created from the pCMV-RGS2-ProLabel-C3 construct cloned previously (Sjögren et al., 2012) using QuikChange II site-directed mutagenesis (Agilent Technologies, Santa Clara, CA) according to the manufacturer's instructions. RGS2-V5 (in pcDNA3.2-DEST) was created by Gateway cloning previously in the laboratory (Phan et al., 2017). K/R mutations were created using QuikChange II site-directed mutagenesis according to the manufacturer's instructions. RGS2-hemagglutinin (HA) and FLAG-FBXO44 [in pF3K WG (BYDV) Flexi] were cloned in-house and used for in vitro transcription/translation. pCMV-HA-FBXO44 was a kind gift from Kevin Glenn, University of Iowa. HA-ubiquitin was a kind gift from Matt Scaglione, Duke University. Primer sequences for construct generation and mutagenesis are available by request.

Antibodies. Rabbit anti-HA (H6908), rabbit anti-FLAG (F7425), mouse anti-FLAG M2 (F1804), mouse anti–β-actin (A2228), rabbit anti–β-actin (A2066), chicken anti-RGS2 (GW22245F), and rabbit anti-FBXO44 (HPA003363) were all from Sigma Aldrich. Chicken anti-HA antibody (ab9111) was from Abcam (Cambridge, MA), and mouse anti-FBXO44 antibody (sc-398020) and mouse anti–α-tubulin (sc-23948) were from Santa Cruz (Santa Cruz, CA). Western blot secondary IRDye 800CW and 680RD antibodies were all from Li-Cor Biosciences (Lincoln, NE). For Western blot experiments, all primary antibodies were diluted 1:1000, and all secondary antibodies were diluted 1:15,000 in Li-Cor blocking buffer supplemented with 0.1% Tween-20.

Cell Culture. Cells were maintained in a humidified incubator at 37°C with 5% CO_2. Human embryonic kidney 293T (HEK-293T) cells were cultured in Dulbecco's modified Eagle's medium (11995; Gibco, Waltham, MA), supplemented with 10% fetal bovine serum (16000; Gibco) and 100 U/ml penicillin with 100 μg/ml streptomycin (15140; Gibco). Human airway smooth muscle cells expressing human telomerase reverse transcriptase, which renders cells senescence resistant (referred to as hTERT cells; Gosens et al., 2006) were maintained and cultured as per Pera and Penn (2019).

Transfections. Cells were transfected with DNA plasmids using Lipofectamine 2000 (Invitrogen) under reduced serum conditions in Opti-MEM (31985; Gibco). Medium was changed to complete culture medium after 4–6 hours, and cells were harvested for experiments 24 hours after transfection.

Small interfering RNA (siRNA) transfections were performed under reduced serum conditions in Opti-MEM 24 hours prior to DNA transfections at 40%–60% confluency. Cells were transfected with siGENOME SMART-POOL siRNA (FBXO44, M-019201-01-0005; Non-Targeting, D-001206-13-05) from Dharmacon (Pittsburgh, PA) using Lipofectamine RNAiMAX (Invitrogen). Experiments were performed 48 hours (HEK-293T) or 72 hours (hTERT) after transfection.

Peptide Synthesis. For each peptide, rink amide LS resin from Creosalus (0.300 mmol/g, 75 mg, 0.0225 mmol, 1 Eq) was swelled in dimethylformamide (DMF) for 45 minutes. The fluorenylmethyloxycarbonyl (Fmoc) was removed with 20% piperidine in DMF for 20 minutes at room temperature (RT) to yield a positive Kaiser test. Fmoc-Met-OH (5 Eq, 0.1125 mmol, 42 mg) and *N,N,N′,N′*-Tetramethyl-*O*-(1*H*-benzotriazol-1-yl)uronium hexafluorophosphate (HBTU) (4.5 Eq, 0.101 mmol, 38 mg) were dissolved in 500 μl DMF. *N,N*-Di-isopropylethylamine (10 Eq, 0.225 mmol, 39 μl) was added, and the amino acid was activated for 2 to 3 minutes before adding to the resin. This was agitated at RT for 30 minutes and checked by Kaiser test, which was negative. This process was repeated for each subsequent amino acid position: for each coupling, the solution was added to the resin's syringe, capped, and agitated for 30 minutes at RT. A Kaiser test was checked after each coupling; if a negative result was not obtained, the coupling reaction was allowed to proceed for an additional 30 minutes. After each amino acid coupling, the Fmoc was removed with 20% piperidine in DMF for 20 minutes at RT to yield a positive Kaiser test. After the final coupling and final Fmoc removal, the resin was washed with DMF (4×), followed by dichloromethane (DCM) (4×).

Peptide was cleaved from resin using 95% trifluoroacetic acid, 2.5% triisopropylsilane, and 2.5% DCM for 2 hours. The solution was collected, and the resin was rinsed with DCM. This solution was then dried by blowing with argon. An ether precipitation was performed twice to obtain a white pellet, which was then dissolved in a mixture of water and acetonitrile with 0.1% trifluoroacetic acid.

All samples were purified by Reverse Phase High-performance liquid chromatography (RP-HPLC) on an Agilent HPLC (1200 series with Agilent Eclipse ZORBAX Bonus-RP, 3.5 μm, 4.6 × 250 mm column; Agilent Technologies). Samples were monitored by UV (210 and 254 nm), and the desired peak was identified using liquid chromatography–mass spectrometry (Agilent 1260 Infinity II with a ZORBAX RR Eclipse Plus C18 3.5 μm, 2.1 × 50 mm column, attached to an Agilent 6129 quadrupole mass spectrometer).

After purification, samples were freeze dried using a ModulyoD lyophilizer (purchased from Savant Instruments, Inc.). All samples had ≥95% purity before use.

Preparation of Cell Lysates. Cells were harvested on ice in radioimmunoprecipitation assay (RIPA) buffer containing protease inhibitors [50 mM Tris-HCl (pH 7.4), 150 mM NaCl, 0.25% w/v deoxycholate, 1 mM EDTA, 1% NP-40, cOmplete Protease Inhibitor Cocktail EDTA-free (Roche, Indianapolis, IN)]. Lysates were bath sonicated for 10 minutes at 4°C and centrifuged at 500*g* for 3 minutes, and the supernatant was used for SDS-PAGE and immunoblotting. Total protein concentration was determined using Pierce BCA Protein Assay Kit (Thermo Scientific). Samples were diluted to 1 μg/μl in protein sample loading buffer (Li-Cor Biosciences).

In Vitro Transcription/Translation. The TNT SP6 High-Yield Wheat Germ Protein Expression System (Promega) was used according to the manufacturer's instructions. Briefly, RGS2-HA and FLAG-FBXO44 [in pF3K WG (BYDV) Flexi] were added to the wheat germ extract, and protein production was allowed proceed to 2 hours at room temperature.

Coimmunoprecipitation. Cells were washed with PBS, then lysed in RIPA buffer containing protease inhibitors for 30 minutes on ice with occasional vortexing. Lysate was centrifuged and supernatant transferred to clean tubes. Samples were incubated with 20 μl protein A agarose beads (Roche) for 30 minutes on rotator at 4°C. Samples were then centrifuged, and the supernatant was used to determine total protein concentration with Pierce BCA Protein Assay Kit (Thermo Scientific). Five hundred micrograms total protein in a volume of 500 μl was used for each immunoprecipitation reaction (1 mg/ml). Twenty microliters was removed from each sample for total input. Three microliters of rabbit anti-HA antibody (H6908; Sigma) was added to each sample prior to incubation on rotator at 4°C overnight. Twenty microliters protein A agarose beads were added to each sample, and samples were then incubated on a rotator at 4°C for 2 hours.

For coimmunoprecipitation (co-IP) using proteins produced by in vitro transcription/translation, equal amounts of reaction mix for RGS2 and FBXO44, respectively, were added to 500 μl RIPA buffer and allowed to form a complex for 1 hour on a rotator at 4°C. Twenty microliters was removed from each sample for total input. Two microliters of mouse anti-FLAG antibody (F1804; Sigma) was added to each sample prior to incubation on rotator at 4°C overnight. Twenty microliters protein G agarose beads (Roche) were added to each sample, and samples were then incubated on a rotator at 4°C for 2 hours.

Samples were centrifuged and supernatant removed. Samples were washed four times with 1 ml RIPA buffer, then once with 1 ml PBS. Bound proteins were eluted from beads at 95°C in 30 μl protein sample loading buffer (Li-Cor Biosciences).

SDS-PAGE and Western Blot. Equal amounts of protein in each lane were resolved on a 12% SDS-PAGE gel for 1 hour at 160 V. Samples were transferred to an Immobilon-FL PVDF membrane (Millipore) and subjected to Western immunoblot analysis using Li-Cor blocking buffer for both blocking and antibody diluents. Membranes were blocked for 1 hour, then incubated for 2 hours in primary antibodies as described under *Antibodies*, and finally incubated for 1 hour with IRDye secondary antibodies directed at the species of the primary antibody. After each antibody incubation, membranes were washed four times in PBS with 0.1% Tween-20. Membranes were imaged using a Li-Cor Odyssey CLx imager. All SDS-PAGE and Western blot experiments were performed and analyzed according to a preset plan.

PathHunter ProLabel Assay. The PathHunter ProLabel assay was run as described previously (Sjögren et al., 2012, 2015). Briefly, transiently transfected HEK-293T cells were plated at 15,000 cells per well in a white, tissue culture-treated 384-well plate (Perkin Elmer) in Dulbecco's modified Eagle's medium without phenol red (21063; Gibco) and 0.5% fetal bovine serum. Cells were allowed to attach overnight followed by treatment with MG-132 at indicated concentrations for 12 hours at 37°C. Prior to detection of RGS2 protein levels by the ProLabel assay, a fluorescent viability assay was performed in the same well. Glycylphenylalanyl-aminofluorocoumarin (GF-AFC) viability substrate (MP Biomedicals, Irvine, CA) was diluted 1:1000 in 100 mM HEPES. Medium was removed from the microplate using an ELx405 CW plate washer (BioTek, Winooski, VT), and 5 μl GF-AFC was added. Plates were incubated at 37°C for 30 minutes; then fluorescence was detected on a Synergy Neo2 multimode plate reader (BioTek). PathHunter ProLabel reagents (DiscoveRx, Fremont, CA) were prepared according to the manufacturer's directions and added to the plate, followed by incubation at room temperature for 3 hours. Luminescence corresponding to RGS2-PL protein levels was detected using a Synergy Neo2 multimode plate reader.

Statistical Analysis. Western blot images were quantified using Image Studio software (Li-Cor Biosciences). Intensity of bands for the protein of interest were normalized to actin as a loading control. Intensity of bands in co-IP experiments were normalized to the input level of the same protein. All data were analyzed using GraphPad Prism 8.0 (GraphPad, La Jolla, CA). Dose response curves were fit using nonlinear regression. Data sets with two groups were analyzed using student's *t* test. Data sets with three or more groups were analyzed with one-way or two-way ANOVA, depending on the nature of the groups as indicated in each figure. Groups were compared with Dunnet's post hoc test for multiple comparisons. All experiments were run at least three times. Data are presented as means ± S.D. with a P value less than 0.05 considered significant.

Results

Alternative Translation Initiation Alters RGS2 Protein Ubiquitination and Degradation. We first aimed to confirm that RGS2 variants resulting from alternative translation initiation were protected from proteasomal degradation. C-terminally FLAG-tagged RGS2 WT and constructs, in which all but one translation initiation site had been mutated to leucine to direct translation initiation (termed M1, M5, M16, or M33, respectively; Fig. 1A), were used to detect effects of proteasome inhibition onRGS2 protein levels. In agreement with previous studies (Kanai et al., 2017), WT, M1, and M5 RGS2 protein levels were significantly increased in transiently transfected HEK-293T cells by the proteasome inhibitor MG-132 (10 μM: Fig. 1, B–D). In contrast, neither M16 nor M33 levels were significantly increased by proteasome inhibition. In addition, the M5 variant expressed at significantly lower levels than WT under basal conditions (14.2% of WT), and the fold increase with MG-132 of M5 trended toward being higher than that of either WT or M1 (Fig. 1D).

Protection from proteasomal degradation could be linked to the inability of the cognate E3 ligase to ubiquitinate RGS2, rendering it nonrecognizable for the proteasome. Therefore, we next determined whether the shorter translation initiation

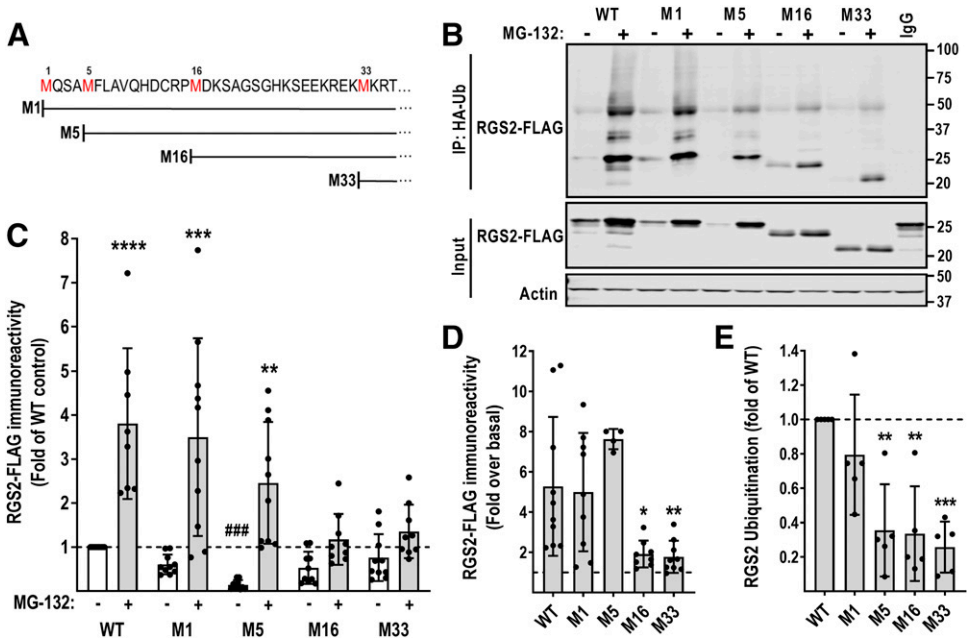

Fig. 1. Effects of alternative translation initiation on RGS2 protein degradation. (A) Schematic representation of RGS2-FLAG with methionine residues that result in alternative translation products highlighted (Met^{1}, Met^{5}, Met^{16}, and Met^{33}). All but one Met was mutated to Leu to drive translation from one specific Met residue (termed M1, M5, M16, or M33, respectively). (B) Representative Western blot demonstrating ubiquitination and MG-132–mediated increases of WT RGS2-FLAG and translation initiation variants. IP, immunoprecipitation; Ub, ubiquitin. (C) WT, M1, and M5 are significantly increased by proteasome inhibition using 10 μM MG-132, whereas the M16 and M33 variants are not. $^{**}P < 0.01$; $^{***}P < 0.001$; $^{****}P < 0.0001$ control vs. MG-132 and $^{\#\#\#}P < 0.001$ WT vs. M5 using two-way ANOVA with Dunnet's post hoc test for pairwise comparisons. (D) The fold increase in RGS2 protein levels is significantly lower for the M16 and M33 variants than for either WT, M1, or M5. (E) Ubiquitination is significantly decreased for the M5, M16, and M33 translation variants, indicating that these variants are less efficiently targeted by an E3 ligase than full-length RGS2. $^{*}P < 0.05$; $^{**}P < 0.01$; $^{***}P < 0.001$ using one one-way ANOVA with Dunnet's post hoc test for pairwise comparisons. Results of five independent experiments run with two technical replicates.

variants displayed alterations in ubiquitination levels. HEK-293T cells were transiently transfected with RGS2-FLAG (WT, M1, M5, M16, or M33) and HA-ubiquitin, then subjected to co-IP utilizing the HA tag on ubiquitin. After MG-132 treatment (10 μM), WT and M1 RGS2-FLAG displayed robust polyubiquitination, in agreement with our previous studies (Sjögren et al., 2015) and the upregulation of these variants by MG-132 (Fig. 1, B and E). The M16 and M33 variants displayed a significant reduction in polyubiquitination levels, indicating that these variants are not being properly targeted by an E3 ligase (Fig. 1, B and E). The M5 variant also displayed significantly reduced ubiquitination; however, this could be the result of very low protein expression levels at baseline. Reduced protein levels of the M5 variant were consistently observed throughout the studies, occasionally interfering with accurate quantification of the Western blot data. This could also explain the reduced observed ubiquitination of the M5 variant, despite it being robustly increased by MG-132.

To further confirm the effect of proteasome inhibition on RGS2 translation initiation variant protein levels, we used an alternative method, the PathHunter ProLabel assay, a high-throughput β-galactosidase complementation assay previously established in the laboratory (Fig. 2) (Sjögren et al., 2012, 2015). Similar to the results using Western blot, M16 and M33 showed a significant reduction in maximum response to MG-132 compared with WT (Fig. 2, C–E). Again, the M5 variant resulted in a trend toward a higher maximum response to MG-132 compared with WT, but the increase was not statistically significant (Fig. 2, B and E). The EC_{50} for MG-132 to increase RGS2 protein levels also trended toward being increased for all translation variants (Fig. 2F), indicating that both potency and efficacy of MG-132 on RGS2 protein levels may be altered by alternative translation initiation.

Determination of the Ubiquitination Site in RGS2. RGS2 consists of 211 amino acids, including 22 lysine residues (K). Four of these are located within the first 33 N-terminal residues and could possibly be affected by alternative translation initiation. To rule out that the decrease in ubiquitination observed in M16 and M33 was due to removal of the lysine crucial for ubiquitination, we analyzed the RGS2 sequence for putative ubiquitination sites using Ub-pred (www.ubpred.org; (Radivojac et al., 2010); Supplemental Table 1). Four putative ubiquitination sites, K^{18}, K^{71}, K^{146}, and K^{200}, were predicted to be sites of ubiquitination. We mutated each of these to arginine (R) in a RGS2-V5 construct. We also included K^{39}, previously hypothesized to be a site of ubiquitination using a different algorithm (Lyu et al., 2015). Removal of K^{200} resulted in complete abolishment of RGS2 ubiquitination (Fig. 3, A and B), suggesting that this residue is the probable ubiquitination site in RGS2. This mutant also displayed higher basal protein expression levels (Fig. 3C), as well as complete abolishment of MG-132–mediated protein upregulation (Fig. 3D), indicating protection from constitutive degradation. This provides evidence that the reduced ubiquitination observed in the M16 and M33 variants (Fig. 1, B and E) is likely not due to the loss of the lysine ubiquitination site; rather it is probable that the N terminus is responsible for recruitment to the cognate E3 ligase.

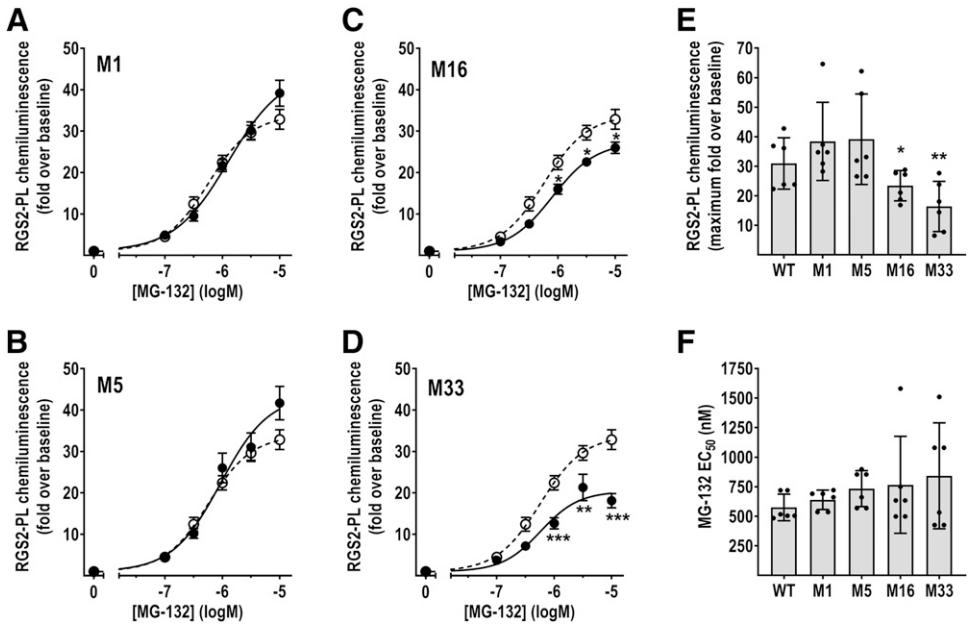

Fig. 2. High-throughput detection of the effects of alternative translation initiation on RGS2 protein degradation. The RGS2 variants (M1, M5, M16, and M33) were created using sequential mutagenesis in the RGS2-PL construct to enable high-throughput detection of changes in RGS2 protein levels. (A–D) HEK-293T cells transiently transfected with RGS2-PL WT (open circles; dashed line) or one of the translation variants (closed circles; solid line) were treated with varying concentrations of MG-132 in 384-well format for 16–18 hours, followed by detection of RGS2-PL label using the PathHunter ProLabel assay. Data were normalized using a concurrent fluorescent viability assay. MG-132 increases all translation variants in a dose-dependent manner. However, M16 and M33 are increased by a significantly lesser extent than WT, M1, or M5. $^{*}P < 0.05$; $^{**}P < 0.01$; $^{***}P < 0.001$ using two-way ANOVA followed by Dunnet's post hoc test for pairwise comparison within rows. (E) The maximum fold increase in response to MG-132 is significantly smaller for M16 and M33 than WT, M1, or M5. $^{*}P < 0.05$; $^{**}P < 0.01$ using one-way ANOVA followed by Dunnet's post hoc test for pairwise comparison. (F) EC_{50} for MG-132–mediated RGS2-PL levels is not significantly altered by alternative translation initiation, although there is a trend toward increased EC_{50} for the shorter variants. Results of six independent experiments run with four technical replicates.

Alternative Translation Initiation Affects RGS2 Targeting by FBXO44. We previously identified a novel cullin-RING E3 ligase capable of degrading RGS2 (Sjögren et al., 2015). E3 ligases recognize their substrates through protein motifs referred to as degrons. These can be short peptide sequences or exposed N termini in the substrate protein. Therefore, we next set out to address whether alternative translation initiation of RGS2 affects target recognition by the

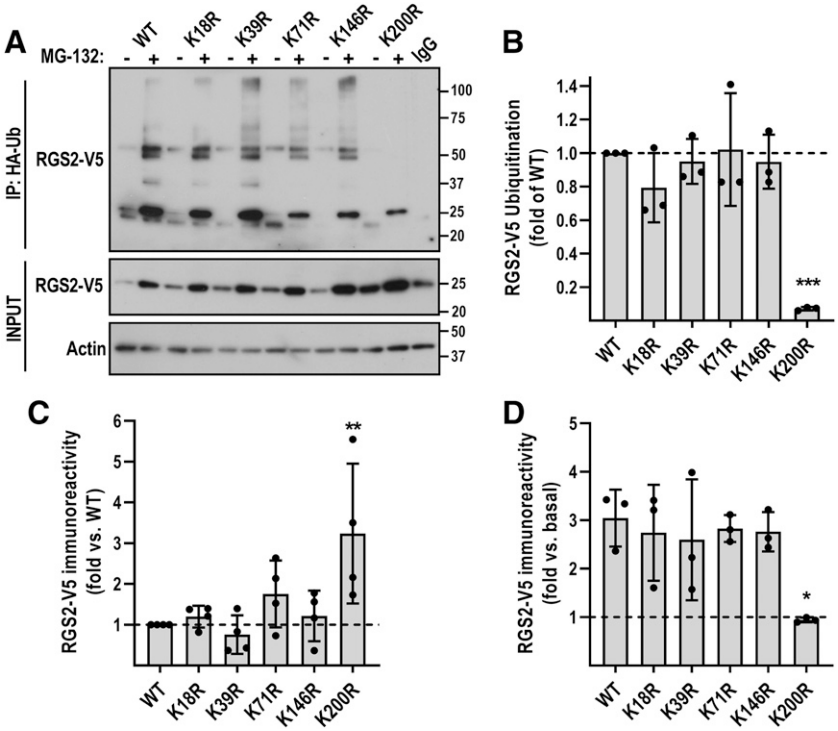

Fig. 3. Determination of the ubiquitination site in RGS2. Four lysine (K) residues in RGS2, K^{18}, K^{71}, K^{146}, and K^{200}, predicted to be sites of ubiquitination (Supplemental Table 1) were mutated to srginine (R). K^{39} was also included, since it has previously been proposed to be a site of ubiquitination using a different algorithm (Lyu et al., 2015). Cells cotransfected with RGS2-V5 WT or K/R mutants and HA-ubiquitin were treated with MG-132 (10 μM; 16–18 hours) to induce RGS2 ubiquitination, followed by co-IP using an anti-HA antibody followed by Western blot analysis of ubiquitinated RGS2-V5. (A) Representative Western blot. (B) Quantification of RGS2 ubiquitination from four independent experiments. RGS2 WT and four out of five mutants are ubiquitinated to a similar level. In contrast, the $K^{200}R$ mutant is not ubiquitinated. IP, immunoprecipitation; Ub, ubiquitin. (C) The $K^{200}R$ mutant displays higher protein levels under basal conditions. (D) $K^{200}R$ is not upregulated by MG-132. $^{*}P < 0.05$; $^{**}P < 0.01$; $^{***}P < 0.001$ using one-way ANOVA followed by Dunnet's post hoc test for pairwise comparison. Results of four independent experiments.

E3 ligase component, FBXO44.To determine whether alternative translation initiation affects how RGS2 is recognized by FBXO44, we used siRNA to knock down endogenous FBXO44 in HEK-293T cells transiently transfected with RGS2-FLAG WT, M1, M5, M16, or M33. On average, we achieved 70% knockdown of FBXO44 (Fig. 4C), and this resulted in a significant increase in both WT and M1 protein levels (Fig. 4, A and B). In contrast, and in agreement with our data using MG-132, M16 and M33 were not increased by FBXO44 knockdown. The M5 variant was also not increased by FBXO44 knockdown, but low overall expression levels of the M5 variant impeded accurate quantification.

To confirm that increased RGS2 protein levels resulting from FBXO44 siRNA knockdown is not due to nonspecific effects of RGS2 overexpression, we next determined the effects of FBXO44 knockdown on endogenous RGS2 protein levels. Immortalized human airway smooth muscle cells (hTERT; kind gift from Raymond Penn, Thomas Jefferson University) expressed both FBXO44 and RGS2 endogenously. siRNA transfection resulted in an almost complete abolishment of FBXO44 protein in these cells (Fig. 4D). Reduced FBXO44 protein levels resulted in a significant increase in RGS2 protein levels, to a similar extent to what was observed in transfected HEK-293T cells (Fig. 4, E and F). This suggests that RGS2 is regulated by FBXO44 in endogenously expressing systems, and not only in transfected cell lines.

We next investigated whether alternative RGS2 translation initiation alters its ability to interact with FBXO44. We performed co-IP between RGS2-FLAG WT and translation initiation variants with HA-FBXO44 in transiently transfected HEK-293T cells. Both WT and M1 RGS2-FLAG was effectively associated with FBXO44 (Fig. 5A). In contrast, and in agreement with our siRNA results, none of the shorter translation variants displayed any interaction with FBXO44 (Fig. 5A). Once again, we observed very low protein levels of the M5 variant, which could possibly explain the lack of association with FBXO44. Overall these data indicate that the degron for FBXO44 consists of a stretch of residues located near the N terminus of RGS2. To further narrow down the region involved in the interaction between RGS2 and FBXO44, we synthesized peptides corresponding to Met^5-Met^{16} and His^{11}-Met^{16}, respectively (termed M^5-M^{16} and H^{11}-M^{16}; Fig. 5B). We next investigated the ability for these peptides to block the interaction between RGS2 and FBXO44 produced by in vitro transcription/translation. In the absence of a peptide, RGS2 and FBXO44 associate in in this setting (Fig. 5B), suggesting a direct interaction between the two proteins, given that the in vitro transcription/translation reactions are void of any mammalian proteins that could serve as adaptors in HEK-293T cells. Both peptides completely blocked this interaction, suggesting that the degron that targets RGS2 for FBXO44-mediated degradation is located between His^{11} and Met^{16}.

Phosphorylation Protects RGS2 from FBXO44-Mediated Proteasomal Degradation. Substrate recognition for F-box proteins can be mediated by post-translational modifications that can either create or destroy degrons. Our data indicate that RGS2 is targeted by FBXO44 through residues in its N terminus. To determine whether post-translational modifications are involved in targeting RGS2 for degradation, we first performed co-IP between RGS2-FLAG and HA-FBXO44 in HEK-293T cell lysates treated with either a phosphatase

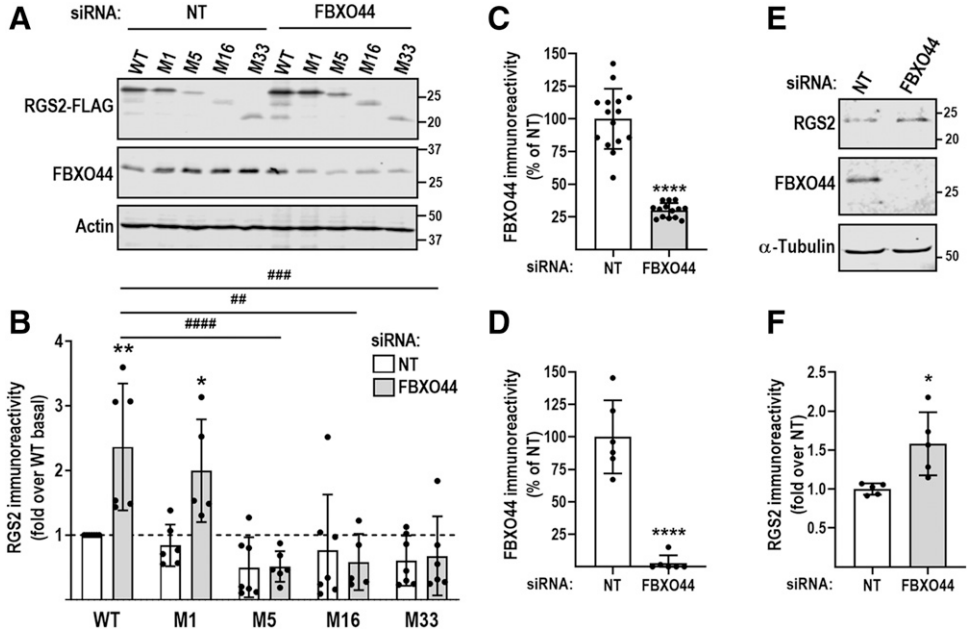

Fig. 4. Alternative RGS2 translation initiation affects FBXO44-mediated degradation. (A) Representative Western blot. (B) Quantification of six independent experiments run with two technical replicates, demonstrating that siRNA-mediated knockdown of FBXO44 increases protein levels of WT and M1 but not M5, M16, or M33 RGS2-FLAG in transiently transfected HEK-293T cells. $^{*}P < 0.05$; $^{**}P < 0.01$ for effects of nontargeting (NT) vs. FBXO44 siRNA FBXO44 siRNA on expression of each variant; $^{\#\#}P < 0.01$; $^{\#\#\#}P < 0.001$; $^{\#\#\#\#}P < 0.0001$ for effects of FBXO44 siRNA on RGS2 fold increase of each variant; both using two-way ANOVA followed by Dunnet's post hoc test for pairwise analysis. (C, D) siRNA-mediated knockdown resulted in an average of 70% reduction of FBXO44 protein levels compared with nontargeting (NT) siRNA in HEK-293T cells (N = 15) (C) and almost complete abolishment of FBXO44 protein expression in human airway smooth muscle cells (hTERT; N = 6) (D). (E, F) Representative Western blot (E) and quantification (F) (N = 6), demonstrating that siRNA-mediated knockdown of FBXO44 increases protein levels of endogenous RGS2 protein levels in hTERT cells. $^{*}P < 0.05$, $^{****}P < 0.0001$ using Student's unpaired t test.

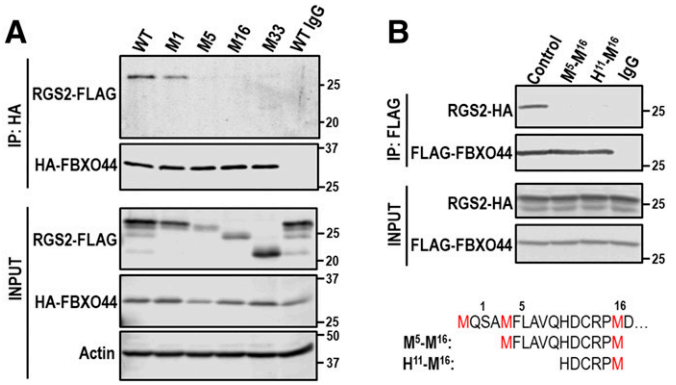

Fig. 5. Effects of alternative RGS2 translation initiation on FBXO44 association. (A) HEK-293T cells transiently transfected with HA-FBXO44 and RGS2-FLAG translation initiation variants were subjected to co-IP using an anti-HA antibody. WT and M1 associates with FBXO44, but the interaction is lost for M5, M16, and M33, indicating that the interaction with FBXO44 is mediated by the N terminus of RGS2. IP, immunoprecipitation. (B) RGS2 and FBXO44 associate in the absence of mammalian adaptor proteins. Peptides (at 100 μM) mimicking residues in the N terminus of RGS2 blocks the association between RGS2-HA and FLAG-FBXO44 proteins produced by in vitro transcription/translation.

inhibitor (sodium orthovanadate) or calf intestinal alkaline phosphatase (CIP). As shown in Fig. 6A, phosphatase inhibition effectively prevented association between RGS2 and FBXO44, whereas CIP treatment resulted in robust association, indicating that phosphorylation may interfere with targeting RGS2 to associate with FBXO44.

To further determine the mechanism by which phosphorylation may interfere with the RGS2-FBXO44 association, we analyzed the RGS2 N-terminal sequence for potential phosphorylation sites using the NetPhos 3.1 phosphorylation site prediction tool (http://www.cbs.dtu.dk/services/NetPhos/; Blom et al., 1999; Supplemental Table 2). Within the first 33 residues, Ser^{3}, Ser^{19}, Ser^{22}, and Ser^{26} were predicted as possible phosphorylation sites. Given that the M5 variant is expressed at lower levels despite having the predicted FBXO44 interaction sequence present, and the lack of FBXO44 association of M16 and M33, we hypothesized that phosphorylation of Ser^{3} may interfere with FBXO44 association. To test this, we mutated Ser^{3} to alanine (S3A) or aspartic acid (S3D) to create nonphosphorylatable and phosphomimetic RGS2, respectively (Fig. 6B). To determine if these mutants alter RGS2 degradation, we transiently transfected HEK-293T cells with RGS2-FLAG (WT, S3A, or S3D) and treated with MG-132. Whereas S3A demonstrated a similar response to MG-132 to that of WT, the phosphomimetic S3D mutation caused a complete suppression of the response to MG-132 (Fig. 6C). In addition, S3A expressed at significantly lower levels than either WT or S3D RGS2 under basal conditions (59.8% and 54.4% of WT and S3D, respectively). Taken together, these data indicate that phosphorylation of Ser^{3} protects RGS2 from proteasomal degradation.

We next determined the effects of the nonphosphorylatable S3A and phosphomimetic S3D mutation on the ability of RGS2 to associate with FBXO44. HEK-293T cells transiently transfected with HA-FBXO44 and RGS2-FLAG (WT, S3A, or S3D) were subjected to co-IP utilizing the HA tag on FBXO44. Although neither mutation completely prevented RGS2 from associating with FBXO44, the S3D mutation caused a significant reduction in the fraction of RGS2-FLAG that was immunoprecipitated (Fig. 6D). In addition, the S3A mutation increased FBXO44 association, although this increase was not statistically significant. Altogether these data indicate that phosphorylation of Ser^{3} may be involved in preventing RGS2 from interacting with FBXO44.

Discussion

Altogether our current study demonstrates that RGS2 is targeted for FBXO44-mediated degradation through an N-terminal degron, located at His^{11}-Met^{16}, which is destroyed by phosphorylation of Ser^{3}. A model for this is presented in Fig. 7. These studies expand on previous observations by us and others (Gu et al., 2008; Sjögren et al., 2015; Kanai et al., 2017) and provide a mechanistic explanation for the increased protein stability that results from alternative translation initiation of RGS2.

Previous studies have indicated that N-terminal residues in RGS2 are important for protein stability and provided an alternative hypothesis for RGS2 degradation. One study suggested that RGS2 can be a target for the N-end rule

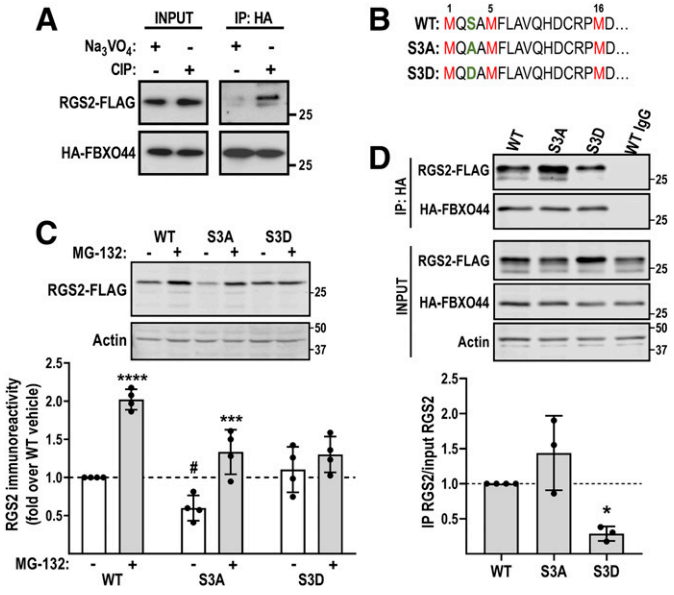

Fig. 6. N-terminal phosphorylation prevents FBXO44-mediated RGS2 degradation. (A) Treatment with CIP promotes strong association between RGS2 and FBXO44, but little to no association is observed in the presence of the phosphatase inhibitor sodium orthovanadate (Na_3VO_4). (B) Schematic of the S3A (phosphodead) and S3D (phosphomimetic) mutations. (C) Representative Western blot and quantified results from four independent experiments demonstrating effects of 4-hour MG-132 treatment (10 μM) on RGS2-FLAG protein levels. S3A expresses at significantly lower basal levels than RGS2 WT. In addition, whereas the protein levels of both RGS2 WT and S3A are significantly increased by MG-132, the S3D mutation blocks MG-132–mediated increases in RGS2 protein levels. $^{*}P < 0.05$; $^{***}P < 0.001$; $^{****}P < 0.0001$ using two-way ANOVA followed by Dunnet's post hoc test for pairwise comparison. Results of three independent experiments run with two technical replicates. (D) The S3D mutation significantly reduces association of RGS2 with FBXO44, as demonstrated by co-IP in cells transiently transfected with HA-FBXO44 and RGS2-FLAG WT, S3A, or S3D. There is also a trend, however not statistically significant, toward increased association of RGS2-S3A and FBXO44. Levels of RGS2 were normalized to input levels, followed by comparison with amount RGS2 WT pulled down. IP, immunoprecipitation. $^{*}P < 0.05$ using one-way ANOVA followed by Dunnet's post hoc test for pairwise comparison. Results of four independent experiments.

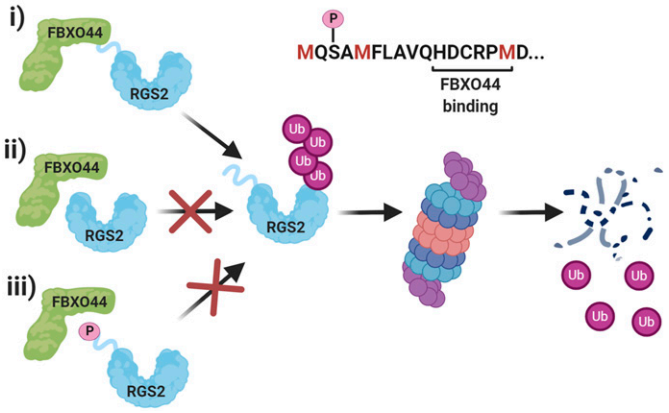

Fig. 7. Model of FBXO44-mediated RGS2 protein degradation. (i) Full-length RGS2 (WT or M1) binds to FBXO44 through its N terminus, facilitating ubiquitination and proteasomal degradation. (ii) In the absence of the first 15 residues (as in the M16 and M33 translation initiation variants), RGS2 does not associate with FBXO44, and ubiquitination and degradation are prevented. (iii) Phosphorylation of Ser^3 of RGS2, as modeled by the S3D mutation, prevents RGS2 from associating with FBXO44, thus inhibiting proteasomal degradation. Image created using Biorender (Biorender.com).

pathway (Park et al., 2015), similar to the closely related RGS4 and 5 (Davydov and Varshavsky, 2000; Lee et al., 2005, 2011). In this model, the N-terminal Gln^2 would be acetylated and targeted by the E3 ligase TEB4 (Park et al., 2015). The Q2L mutation found in hypertensive patients (Yang et al., 2005) causes destabilization of RGS2 (Bodenstein et al., 2007) and, according to this proposed model, this is due to dual targeting by both the acetylation and arginylation arm of the N-end rule pathway. Arginylation, the mechanism by which RGS4 and RGS5 are targeted (Davydov and Varshavsky, 2000; Lee et al., 2011), is mediated by arginyl transferase, which is encoded by *ATE-1*. We have, however, been unable to confirm these findings. In fact, in our previous studies, we demonstrated that siRNA-mediated knockdown of ATE-1, although it significantly stabilized RGS4, had no effect on RGS2-Q2L protein expression (Sjögren et al., 2015). In addition, a recent study failed to confirm association between RGS2 and TEB4 (Kanai et al., 2017). Instead, we identified an alternative pathway for RGS2 protein degradation, mediated by FBXO44 (Sjögren et al., 2015). Although our model of FBXO44-mediated RGS2 protein degradation includes a degron at the very N terminus of RGS2, it does not seem that RGS2 is a substrate for the N-end rule pathway, at least in our hands. Based on our current data, however, we cannot rule out other potential degradation mechanisms for RGS2. Ubiquitination of the M16 and M33 variant, albeit significantly reduced, is not completely abolished. Hence, there may be alternative mechanisms involved in RGS2 ubiquitination and degradation, which are not dependent on the presence of the initial 16 residues. Nevertheless, in our hands it seems that FBXO44-mediated targeting of RGS2 for degradation is a major pathway.

Our present data and previous studies (Kanai et al., 2017) indicate that the M5 translation initiation variant is degraded at a faster rate than full-length RGS2. Throughout these studies, we consistently observed low expression levels of the M5 variant, sometimes impeding accurate quantification of Western blot data. The hydrophobic degradation signal near the N terminus previously identified (residues ^{6}FLAV^9; Kanai et al., 2017) is preserved in this variant, and the molecular basis for enhanced degradation has not been previously explained. Our determination that phosphorylation of Ser^3 prevents RGS2 from binding FBXO44 and protects RGS2 from proteasomal degradation (Fig. 6) provides an explanation for the destabilization of the M5 variant. The identity of the kinase responsible for this phosphorylation is currently unknown. We previously demonstrated that activation of protein kinase C (PKC) leads to increased RGS2 protein levels, serving as a negative feedback mechanism for Gq-mediated signaling (Raveh et al., 2014). At that time, it was not clear whether the effect on RGS2 protein levels was through direct phosphorylation by PKC, but our current data open up the possibility that PKC-mediated phosphorylation of RGS2 serves to protect it from being degraded by FBXO44. Ongoing studies in the laboratory are aimed at deciphering these mechanisms.

F-box proteins are a 69-member family of CRL E3 ligase substrate-recognition components, previously proposed as targets to afford better selectivity in UPS inhibition (Wang et al., 2014). For the majority of F-box proteins, little is known about substrate specificity, which presents an obstacle to drug design. FBXO44 is one of the least characterized F-box proteins. It is closely homologous to a group of F-box proteins recruiting proteoglycans as substrates. However, despite the fact that the sugar-binding residues are preserved, FBXO44 does not bind to the same substrates (Glenn et al., 2008). A recent comparison of the crystal structures of FBXO44 and F-box only protein 2 in complex with the adaptor protein S-phase kinase-associated protein 1 (Skp1) (Kumanomidou et al., 2015) provided a molecular basis for FBXO44 substrate selectivity. Substrate binding for both proteins were mapped to the loops linking the antiparallel β strands that make up the F-box–associated domain. These loops show the greatest variability between FBXO44 and F-box only protein 2 and drive substrate selectivity. In addition, although the F-box domain is fairly conserved between the two proteins, binding to Skp1 induces different conformations, which may also impact substrate selectivity. Our previous observation that FBXO44 only degrades RGS2 in the context of a cullin 4B–DNA damage-binding protein 1 complex, but not when associated with cullin 1–Skp1 (Sjögren et al., 2015), provides further indications about the dynamic nature of this poorly characterized F-box protein. Apart from RGS2, FBXO44 also recognizes breast cancer type 1 susceptibility protein (BRCA1) as its only other known substrate (Lu et al., 2012). In contrast to RGS2, FBXO44-mediated BRCA1 degradation occurs in the context of a cullin 1–Skp1 complex. Thus, FBXO44 substrate selectivity may be directed by the nature of the associated CRL complex.

In conclusion, in the current study, we identified a molecular basis for RGS2 to be targeted for FBXO44-mediated degradation. These studies shed further light on the intricate mechanisms involved in regulating RGS2 protein levels. It also brings us one step closer to enabling rational drug design of RGS2 protein stabilizing compounds that would be promising therapeutic leads in diseases associated with destabilized RGS2 protein levels, including hypertension, heart failure, and anxiety. Furthermore, if such compounds are specific inhibitors of the RGS2-FBXO44 interaction, BRCA1 and any yet-to-be-discovered FBXO44 substrates would be unaffected.

For this approach to be feasible, however, further studies are warranted to determine the structural basis for FBXO44 binding to RGS2 and BRCA1, respectively.

Acknowledgments

The authors would like to thank Kendall Blumer (Washington University School of Medicine), Kevin Glenn (University of Iowa), and Matt Scaglione (Duke University) for kindly supplying some of the DNA constructs used in the present study. We also thank Raymond Penn (Thomas Jefferson University) for kindly supplying the hTERT cells.

Authorship Contributions

Participated in research design: McNabb, Sjögren.

Conducted experiments: McNabb, Gonzalez, Muli, Sjögren.

Performed data analysis: McNabb, Gonzalez, Sjögren.

Wrote or contributed to the writing of the manuscript: McNabb, Muli, Sjögren.

References

Adams J (2004) The development of proteasome inhibitors as anticancer drugs. *Cancer Cell* **5**:417–421.

Adams J, Palombella VJ, Sausville EA, Johnson J, Destree A, Lazarus DD, Maas J, Pien CS, Prakash S, and Elliott PJ (1999) Proteasome inhibitors: a novel class of potent and effective antitumor agents. *Cancer Res* **59**:2615–2622.

Blazer LL, Roman DL, Chung A, Larsen MJ, Greedy BM, Husbands SM, and Neubig RR (2010) Reversible, allosteric small-molecule inhibitors of regulator of G protein signaling proteins. *Mol Pharmacol* **78**:524–533.

Blazer LL, Zhang H, Casey EM, Husbands SM, and Neubig RR (2011) A nanomolar-potency small molecule inhibitor of regulator of G-protein signaling proteins. *Biochemistry* **50**:3181–3192.

Blom N, Gammeltoft S, and Brunak S (1999) Sequence and structure-based prediction of eukaryotic protein phosphorylation sites. *J Mol Biol* **294**:1351–1362.

Bodenstein J, Sunahara RK, and Neubig RR (2007) N-terminal residues control proteasomal degradation of RGS2, RGS4, and RGS5 in human embryonic kidney 293 cells. *Mol Pharmacol* **71**:1040–1050.

Cao X, Qin J, Xie Y, Khan O, Dowd F, Scofield M, Lin MF, and Tu Y (2006) Regulator of G-protein signaling 2 (RGS2) inhibits androgen-independent activation of androgen receptor in prostate cancer cells. *Oncogene* **25**:3719–3734.

Ciechanover A and Schwartz AL (2002) Ubiquitin-mediated degradation of cellular proteins in health and disease. *Hepatology* **35**:3–6.

Davydov IV and Varshavsky A (2000) RGS4 is arginylated and degraded by the N-end rule pathway in vitro. *J Biol Chem* **275**:22931–22941.

Ding Q, Zhang Z, Liu JJ, Jiang N, Zhang J, Ross TM, Chu XJ, Bartkovitz D, Podlaski F, Janson C, et al. (2013) Discovery of RG7388, a potent and selective p53-MDM2 inhibitor in clinical development. *J Med Chem* **56**:5979–5983.

George T, Chakraborty M, Giembycz MA, and Newton R (2018) A bronchoprotective role for *Rgs2* in a murine model of lipopolysaccharide-induced airways inflammation. *Allergy Asthma Clin Immunol* **14**:40.

Glenn KA, Nelson RF, Wen HM, Mallinger AJ, and Paulson HL (2008) Diversity in tissue expression, substrate binding, and SCF complex formation for a lectin family of ubiquitin ligases. *J Biol Chem* **283**:12717–12729.

Gosens R, Stelmack GL, Dueck G, McNeill KD, Yamasaki A, Gerthoffer WT, Unruh H, Gounni AS, Zaagsma J, and Halayko AJ (2006) Role of caveolin-1 in p42/p44 MAP kinase activation and proliferation of human airway smooth muscle. *Am J Physiol Lung Cell Mol Physiol* **291**:L523–L534.

Gu S, Anton A, Salim S, Blumer KJ, Dessauer CW, and Heximer SP (2008) Alternative translation initiation of human regulators of G-protein signaling-2 yields a set of functionally distinct proteins. *Mol Pharmacol* **73**:1–11.

Herrmann J, Ciechanover A, Lerman LO, and Lerman A (2004) The ubiquitin-proteasome system in cardiovascular diseases-a hypothesis extended. *Cardiovasc Res* **61**:11–21.

Hershko A and Ciechanover A (1998) The ubiquitin system. *Annu Rev Biochem* **67**: 425–479.

Heximer SP, Knutsen RH, Sun X, Kaltenbronn KM, Rhee MH, Peng N, Oliveira-dos-Santos A, Penninger JM, Muslin AJ, Steinberg TH, et al. (2003) Hypertension and prolonged vasoconstrictor signaling in RGS2-deficient mice. *J Clin Invest* **111**: 445–452.

Hoeller D, Hecker CM, and Dikic I (2006) Ubiquitin and ubiquitin-like proteins in cancer pathogenesis. *Nat Rev Cancer* **6**:776–788.

Holden NS, Bell MJ, Rider CF, King EM, Gaunt DD, Leigh R, Johnson M, Siderovski DP, Heximer SP, Giembycz MA, et al. (2011) β2-Adrenoceptor agonist-induced RGS2 expression is a genomic mechanism of bronchoprotection that is enhanced by glucocorticoids. *Proc Natl Acad Sci USA* **108**:19713–19718.

Kanai SM, Edwards AJ, Rurik JG, Osei-Owusu P, and Blumer KJ (2017) Proteolytic degradation of regulator of G protein signaling 2 facilitates temporal regulation of $G_{q/11}$ signaling and vascular contraction. *J Biol Chem* **292**:19266–19278.

Kumanomidou T, Nishio K, Takagi K, Nakagawa T, Suzuki A, Yamane T, Tokunaga F, Iwai K, Murakami A, Yoshida Y, et al. (2015) The structural differences between a glycoprotein specific F-box protein Fbs1 and its homologous protein FBG3. *PLoS One* **10**:e0140366.

Lee MJ, Tasaki T, Moroi K, An JY, Kimura S, Davydov IV, and Kwon YT (2005) RGS4 and RGS5 are in vivo substrates of the N-end rule pathway. *Proc Natl Acad Sci USA* **102**:15030–15035.

Lee PC, Sowa ME, Gygi SP, and Harper JW (2011) Alternative ubiquitin activation/conjugation cascades interact with N-end rule ubiquitin ligases to control degradation of RGS proteins. *Mol Cell* **43**:392–405.

Lu Y, Li J, Cheng D, Parameswaran B, Zhang S, Jiang Z, Yew PR, Peng J, Ye Q, and Hu Y (2012) The F-box protein FBXO44 mediates BRCA1 ubiquitination and degradation. *J Biol Chem* **287**:41014–41022.

Lyu JH, Park DW, Huang B, Kang SH, Lee SJ, Lee C, Bae YS, Lee JG, and Baek SH (2015) RGS2 suppresses breast cancer cell growth via a MCPIP1-dependent pathway. *J Cell Biochem* **116**:260–267.

Oliveira-Dos-Santos AJ, Matsumoto G, Snow BE, Bai D, Houston FP, Whishaw IQ, Mariathasan S, Sasaki T, Wakeham A, Ohashi PS, et al. (2000) Regulation of T cell activation, anxiety, and male aggression by RGS2. *Proc Natl Acad Sci USA* **97**: 12272–12277.

Park EJ, Choi KS, Yoo YH, and Kwon TK (2013) Nutlin-3, a small-molecule MDM2 inhibitor, sensitizes Caki cells to TRAIL-induced apoptosis through p53-mediated PUMA upregulation and ROS-mediated DR5 upregulation. *Anticancer Drugs* **24**: 260–269.

Park SE, Kim JM, Seok OH, Cho H, Wadas B, Kim SY, Varshavsky A, and Hwang CS (2015) Control of mammalian G protein signaling by N-terminal acetylation and the N-end rule pathway. *Science* **347**:1249–1252.

Pera T and Penn RB (2019) Methods to investigate β-arrestin-mediated regulation of GPCR function in human airway smooth muscle. *Methods Mol Biol* **1957**:69–82.

Phan HTN, Sjögren B, and Neubig RR (2017) Human missense mutations in regulator of G protein signaling 2 affect the protein function through multiple mechanisms. *Mol Pharmacol* **92**:451–458.

Pickart CM (2001) Mechanisms underlying ubiquitination. *Annu Rev Biochem* **70**: 503–533.

Radivojac P, Vacic V, Haynes C, Cocklin RR, Mohan A, Heyen JW, Goebl MG, and Iakoucheva LM (2010) Identification, analysis, and prediction of protein ubiquitination sites. *Proteins* **78**:365–380.

Raveh A, Schultz PJ, Aschermann L, Carpenter C, Tamayo-Castillo G, Cao S, Clardy J, Neubig RR, Sherman DH, and Sjögren B (2014) Identification of protein kinase C activation as a novel mechanism for RGS2 protein upregulation through phenotypic screening of natural product extracts. *Mol Pharmacol* **86**:406–416.

Ravid T and Hochstrasser M (2008) Diversity of degradation signals in the ubiquitin-proteasome system. *Nat Rev Mol Cell Biol* **9**:679–690.

Ross EM and Wilkie TM (2000) GTPase-activating proteins for heterotrimeric G proteins: regulators of G protein signaling (RGS) and RGS-like proteins. *Annu Rev Biochem* **69**:795–827.

Sjögren B (2017) The evolution of regulators of G protein signalling proteins as drug targets - 20 years in the making: IUPHAR Review 21. *Br J Pharmacol* **174**: 427–437.

Sjögren B, Blazer LL, and Neubig RR (2010) Regulators of G protein signaling proteins as targets for drug discovery. *Prog Mol Biol Transl Sci* **91**:81–119.

Sjögren B, Parra S, Atkins KB, Karaj B, and Neubig RR (2016) Digoxin-mediated upregulation of RGS2 protein protects against cardiac injury. *J Pharmacol Exp Ther* **357**:311–319.

Sjögren B, Parra S, Heath LJ, Atkins KB, Xie ZJ, and Neubig RR (2012) Cardiotonic steroids stabilize regulator of G protein signaling 2 protein levels. *Mol Pharmacol* **82**:500–509.

Sjögren B, Swaney S, and Neubig RR (2015) FBXO44-mediated degradation of RGS2 protein uniquely depends on a cullin 4B/DDB1 complex. *PLoS One* **10**:e0123581.

Tsang S, Woo AY, Zhu W, and Xiao RP (2010) Deregulation of RGS2 in cardiovascular diseases. *Front Biosci (Schol Ed)* **2**:547–557.

Turner EM, Blazer LL, Neubig RR, and Husbands SM (2012) Small molecule inhibitors of regulator of G protein signalling (RGS) proteins. *ACS Med Chem Lett* **3**:146–150.

Wang Z, Liu P, Inuzuka H, and Wei W (2014) Roles of F-box proteins in cancer. *Nat Rev Cancer* **14**:233–247.

Yang J, Kamide K, Kokubo Y, Takiuchi S, Tanaka C, Banno M, Miwa Y, Yoshii M, Horio T, Okayama A, et al. (2005) Genetic variations of regulator of G-protein signaling 2 in hypertensive patients and in the general population. *J Hypertens* **23**: 1497–1505.

Address correspondence to: Benita Sjögren, Department of Medicinal Chemistry and Molecular Pharmacology, Purdue University, 575 West Stadium Mall Drive, West Lafayette, IN 47907. E-mail: jsjogren@purdue.edu